FPGA-Based Broken Bars Detection on Induction Motors Under Different Load Using Motor Current Signature Analysis and Mathematical Morphology

Jose de Jesus Rangel-Magdaleno, *Member, IEEE*, Hayde Peregrina-Barreto, *Member, IEEE*, Juan Manuel Ramirez-Cortes, *Senior Member, IEEE*, Pilar Gomez-Gil, *Senior Member, IEEE*, and Roberto Morales-Caporal, *Member, IEEE*

***Abstract*— Broken bars detection on induction motors has been a topic of interest in recent years. Its detection is important due to the fact that the failure is silent and the consequences it produces as power consumption increasing, vibration, introduction of spurious frequencies in the electric line, among others, can be catastrophic. In this paper, the use of motor current signature analysis and mathematical morphology to detect broken bars on induction motors under different mechanical load condition is analyzed. The proposed algorithm first identifies the motor load and then the motor condition. The statistical analysis of several tests under different motor loads (100%, 75%, 50%, and 25%) and motor condition (healthy, one broken bar, and two broken bars) is presented. The proposed method has been implemented in a field programmable gate array, to be used in real-time online applications. The algorithm obtained in average a 95% accuracy of failure detection.**

***Index Terms*— Broken bars, fault diagnosis, field programmable gate array (FPGA), mathematical morphology, MCSA.**

I. Introduction

ONLINE monitoring systems for early failure detection are a current demand in many industrial areas. In the vast field of rotating machines, induction motors are extensively used for a variety of industrial applications, representing around 85% of worldwide power consumption. Owing to that extensive use, induction motor failure detection has attracted attention from several research groups around the world. Among several faults that can occur in induction machines, broken bars may cause excessive vibrations and higher thermal stress with catastrophic consequences if the situation is not corrected in early stages. In consequence, broken bars detection must be carried out in early stages and under different load conditions [1]. Induction motor analysis can be performed on and offline, resulting in higher interest online analysis because it avoids the shutdown of production lines. Several methodologies for online induction motor broken rotor bars detection have been proposed. Among the most common technique are the analysis of current [1]–[15], vibrations [16]–[20], combinations of current and vibrations [21], [22], voltage [23], [24], and magnetic flux [25]. Motor current signature analysis (MCSA) is one of the most effective techniques for induction motor failure detection [22]. Several methodologies for broken bar detection using MCSA have been proposed. For example, Garcia-Perez *et al*. [6] developed an experimental study for partially broken rotor bar detection using high-resolution spectral analysis. Rangel-Magdaleno *et al.* [8] proposed the use of mathematical morphology (MM) to improve MCSA, where the advantages of using this transformation are presented. Their methodology was applied to a healthy motor and a motor with two broken bars under full-load conditions [8]. Puche-Panadero *et al*. [2] proposed a methodology related to MCSA improvement, where they developed an advanced signal-and-data-processing algorithm based on Hilbert transform of the MCSA for resolution improvement. Toscani *et al*. [1] presented a new fault indicator which is fairly less sensitive to mechanical load based on current and voltage analysis than other techniques. Cusido *et al*. [3] analyzed the motor current using a new specific wavelet-based Agnesi's function to identify the fault frequency component in induction motors. Their technique was verified in stationary and nonstationary motor conditions. Jawadekar *et al*. [4] presented an application based on discrete wavelet transform and artificial neural network for fault detection on induction motors. In their study, the superiority of Db4 wavelet over other standard wavelets for accurate fault classification on induction motors is demonstrated. Pineda-Sanchez *et al*. [5] proposed the use of fractional Fourier transform to perform MCSA during the transient regime. Hu *et al.* [15] developed a novel transform demodulation algorithm that transforms the three-phase currents into a magnetic torque,and the authors demonstrated that using the new transform is possible to extract more detailed fault signature frequency components. Cristaldi *et al*. [11] developed a virtual instrument for monitoring and diagnostic technique of induction motor based on the current peak modulation. Riera-Guasp *et al*. [12]

Manuscript received June 12, 2013; revised September 23, 2013; accepted September 26, 2013. Date of publication January 22, 2014; date of current version April 3, 2014. The Associate Editor coordinating the review process was Dr. Edoardo Fiorucci.

J. de J. Rangel-Magdaleno, J. M. Ramirez-Cortes, and P. Gomez-Gil, are with the National Institute for Astrophysics, Optics and Electronics, Puebla 72840, Mexico (e-mail: jrangel@inaoep.mx; jmram@inaoep.mx; pgomez@inaoep.mx).

H. Peregrina-Barreto is with the Laboratorio de Investigación en Control Reconfigurable A.C., Queretaro 76209, Mexico (e-mail: hperegrina@ieee.org).

R. Morales-Caporal is with the Instituto Tecnologico de Apizaco, Tlax 90300, Mexico (e-mail: rmcaporal@ieee.org).

Color versions of one or more of the figures in this paper are available online at http://ieeexplore.ieee.org.

Digital Object Identifier 10.1109/TIM.2013.2286931

proposed a time–frequency analysis of the transient current based on Gabor analysis, Gaussian window and a detection lattice. Ebrahimi *et al.* [13] proposed a new analytical method for Ohmic and core losses calculation in faulty induction motors; new coefficients were proposed to consider nonsinusoidal distribution effects of flux density due to broken bars. According to cited works, the development of new processing algorithms using MCSA is currently a continuous topic of interest.

Broken rotor bar induction motor failure produces spurious frequencies around the supply frequency (60 Hz in Mexico). MCSA allows the observation of those spurious spectral components with amplitude proportional to the severity the failure. However, for early stage and low-load condition, the detection by an automatic system is difficult.

In this paper, a field programmable gate array (FPGA)-based methodology for broken rotor bar detection under different load condition using MCSA and MM is presented. The proposed methodology is an extension of the algorithm presented in [8], with an improvement on detectability through the addition of a load condition detection module based on a segmentation of the analysis area. To demonstrate the efficiency of the proposed methodology, several tests were performed. Our experiment includes samples with 25%, 50%, 75%, and 100% of load level, and three motor conditions: healthy motors, motors with one broken bar, and motors with two broken bars.

The rest of this paper is organized as follows. Section II presents the theoretical background of MM and an MCSA analysis; the proposed methodology is described in Section III; Section IV shows analysis and, the results on several cases of study. A summary is presented in Section V and Section VI presents the conclusion.

II. MM and MCSA Analysis

Mathematical morphology is a theory and technique originally developed to be used in binary image processing. Further, it was extended to grayscale images and functions. MM has provided an approach to the development of nonlinear signal-processing techniques, where the shape information of a given signal is modified through its interaction with another function called a structuring element (SE). Dilation (δ) and erosion (ε) are the basic morphological operations of MM. The erosion of $f(n)$ by $\mu E(n)$ is represented by $\varepsilon_{\mu E}[f(n)] = f(n)\Theta\mu E(n)$, and it is defined as

$$f(n)\Theta\mu E(n) = \min_{m=0..M-1} \{f(n+m) - \mu E(m)\} \quad (1)$$

where $f(n)$ denotes a discrete signal of length N, and $\mu E(n)$ denotes a symmetric function of length M representing the SE of size μ, with $M = 2\mu + 1$ and typical sizes $N \gg$ M. In a similar way, the dilation of $f(n)$ by $\mu E(n)$, which corresponds to the dual operator of erosion, is represented by $\delta_{\mu E}[f(n)] = f(n) \oplus \mu E(n)$, and it is defined as

$$f(n) \oplus \mu E(n) = \max_{m=0..M-1} \{f(n+m) + \mu E(m)\}. \quad (2)$$

Fig. 1 shows an example of the operations involved in a morphological transformation of time signal $f(n)$ dilated through the use of a SE of size $\mu = 2$. When the SE is located in the n position, the values of the original function $f(n)$ inside a window of size $M = 5$ are analyzed, looking for the maximum value among the positions $n-2$, $n-1$, n, $n+1$, $n+2$. In that example, the maximum value at that point is located in $n+2$, so the dilated signal assumes at the n time the value of the function at $n+2$. Next, the SE is shifted to locate its center at the position $n+1$ and the process is repeated. It can be noticed that erosion and dilation are transformations that allow to eliminate or to remark specific components in the signal according to the size of the transformation [26], [27].

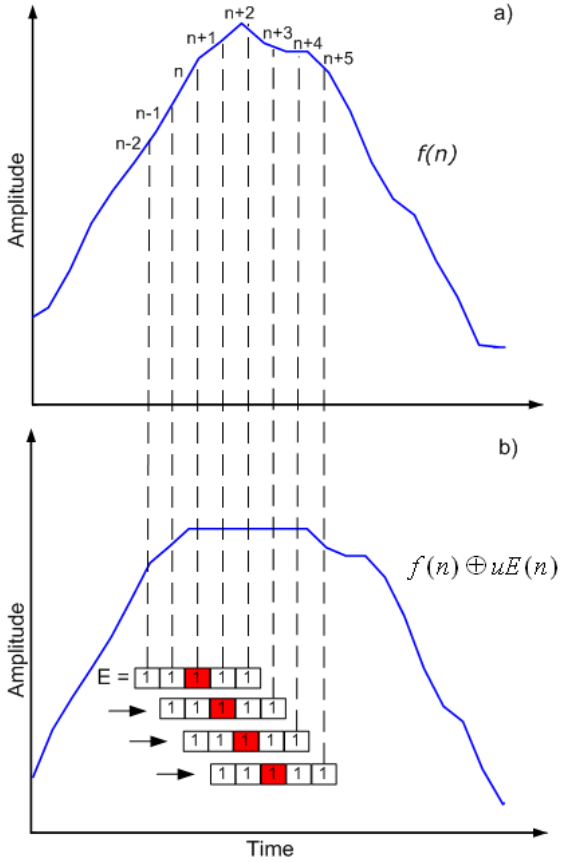

Fig. 1. Time signal (a) original and (b) processed by mathematical morphology operator (dilation) size five.

There are some works using MM for signal processing applied to power systems, recently reported. Radil *et al.* [28] used the MM closing operator for a power quality monitoring system. Jing *et al.* [29] proposed the use of MM as a failure classification on power transformers. In this paper, the use of dilation transformation in current signal allows to remark the broken bars effect in time signal, meanwhile, in frequency domain some low frequencies are remarkable.

As demonstrated in [23], spurious frequencies around the main frequency can be observed in a failure motor, and also in its harmonic frequencies. These frequencies are given by

$$f_{bb} = [h/p(1-s) \pm s] f_s \quad (3)$$

where f_{bb} is the spurious frequency, p is the pair of poles, s is the asynchronous slip between the mechanical speed and the rotating speed, f_s is the supply frequency, and h is an index which indicates the number of harmonics.

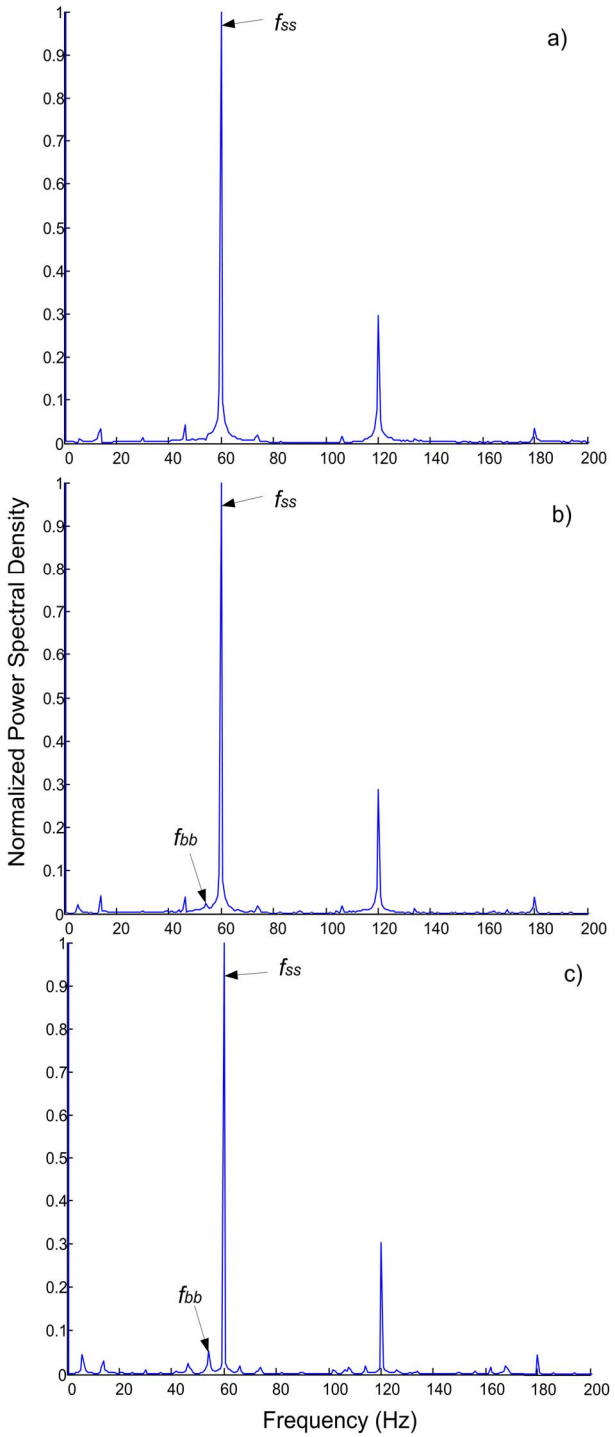

Fig. 2. Power spectral density for (a) healthy motor, (b) motor with one broken bar, and (c) motor with two broken bars.

Fig. 2 shows the power spectral density obtained from three motor conditions: healthy, one broken bar, and two broken bar. Although it is possible to distinguish visually the amplitude of f_{bb} in the case of two broken bars, a statistical analysis based on the amplitude of the spurious frequencies reveals that the frequency of the spectral component has a value very close to the fundamental frequency, which makes its detection difficult through an automatic algorithm. For this reason, the analysis of some new frequency regions have been recently proposed [8], [21], [23].

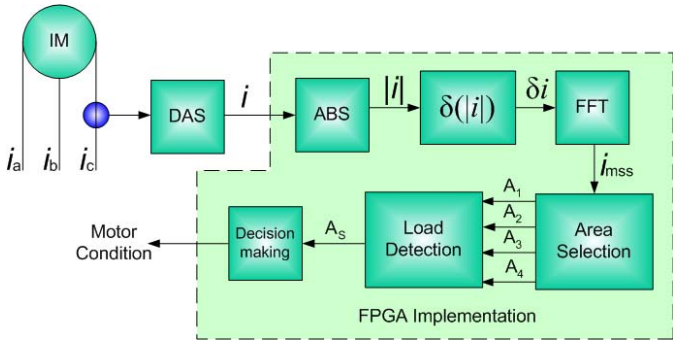

Fig. 3. Proposed methodology.

III. Methodology

The proposed methodology is based on MCSA and MM. This methodology was implemented into a low-cost FPGA from Altera (DE0 nano-development kit) with an operation frequency of 50 MHz. The use of the FPGA allows a real-time low-cost implementation with the advantage of low-power consumption and rapid prototyping. The FPGA implementation reconfigurability provides constant updating to accomplish new requirements, an open architecture for future module integration or improvements in the methodology, and a parallel structure for a fast and efficient processing that permits continuous online monitoring.

Fig. 3 shows the proposed methodology, where the FPGA implementation is bounded by a dotted line. The current signal of one motor phase is obtained using a standard AC current clamp i200s Fluke. The analog signal from clamp is amplified and then converted into a digital signal using a 16-bit analog to digital converter (ADS7809) with sampling rate of 100 kHz configured to work at 1500 Hz. The data acquisition system is controlled by an FPGA, which receives and stores the digital signal to be processed. Next is a description of each step.

1) Acquisition and storage of the current signal.
2) Calculation of the absolute of the signal ($|i|$). This is recommended by [28], to apply a MM operation.
3) A dilation transformation is applied to the absolute value of the signal using a structural element equal to five; in this process the dilation of the current δ_i is obtained.
4) The power spectral density called i_{mss} of the signal is obtained using a 1024-point FFT.
5) The absolute of the power spectral signal i_{mss} is calculated by the block FFT.

Fig. 4 shows the power spectral density of the signal i_{mss} for three different motor conditions: healthy [Fig. 4(a)], one broken bar [Fig. 4(b)], and two broken bars [Fig. 4(c)]. In this figure, the analysis area is marked by a red rectangle; the broken bar frequency is named f_b. In Fig. 4, it can be seen how the amplitude of the frequency (f_b) increases with the damage. A comparison with typical area of analysis, specifically frequency (f_b) with frequency (f_{bb}), shows bigger amplitude of f_b allowing better detection by an automatic system. For an automatic analysis of the motor condition just the new area (marked by a red rectangle) is processed.

6) Area selection unit selects the low frequencies from analysis area (1–10 Hz), then divides the selection in

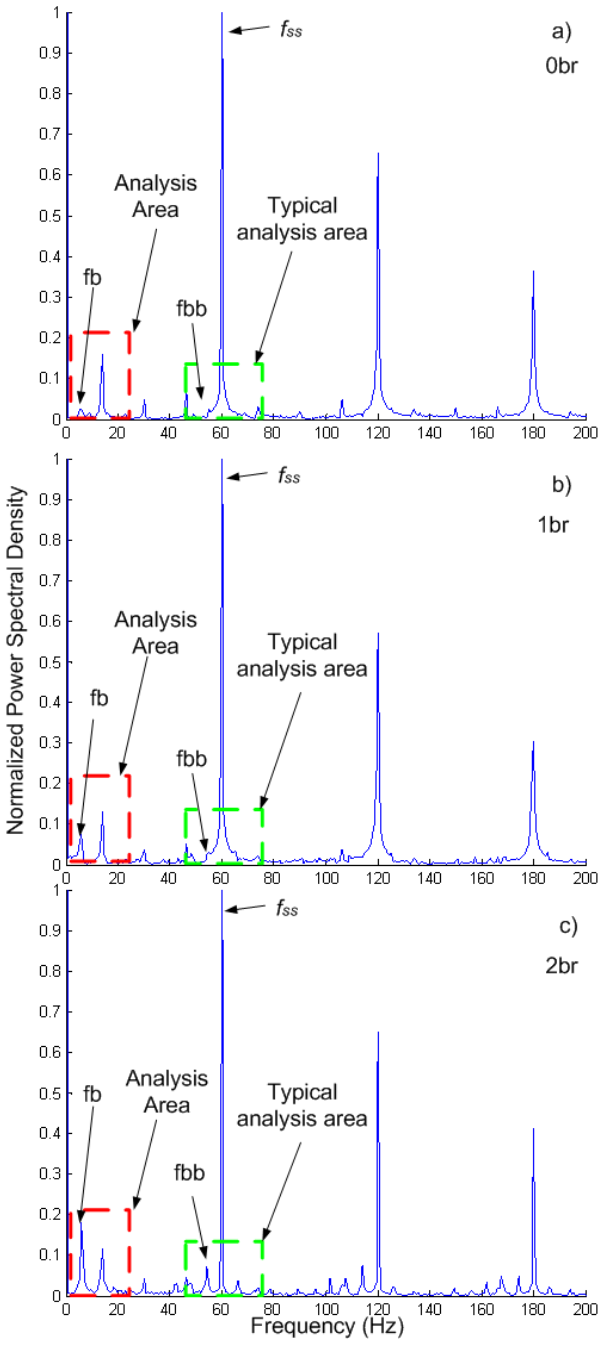

Fig. 4. Power spectral density for current signal under different conditions. (a) Healthy motor. (b) One broken bar. (c) Two broken bars.

four areas, A_1, A_2, A_3, and A_4 whose amplitudes are calculates as

$$A_1 = \sum_{j=3}^{5} i_{\text{mss}}(k) \quad A_2 = \sum_{j=5}^{7} i_{\text{mss}}(k)$$
$$A_3 = \sum_{j=7}^{8} i_{\text{mss}}(k) \quad A_4 = \sum_{j=8}^{10} i_{\text{mss}}(k) \tag{4}$$

where i_{mss} is the power spectral density of the current and k is an index which indicates the points of the power spectral density vector i_{mss} to be analyzed within each area.

7) To determine a load condition, a comparison of the resultant magnitude of the sum of components of these four areas is carried out. The selected segment A_s is obtained as

$$A_s = \max(A_1, A_2, A_3, A_4). \tag{5}$$

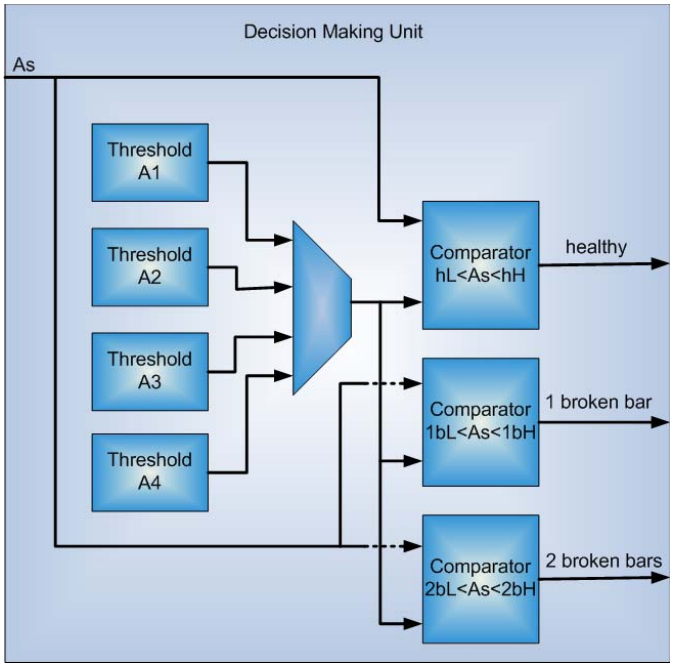

Fig. 5. Decision-making unit.

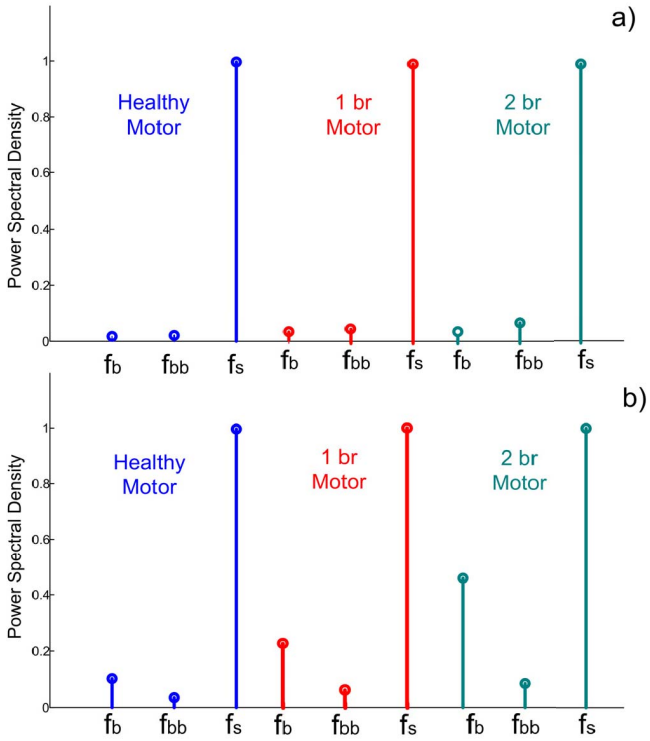

Fig. 6. Frequencies amplitude for healthy motor, motor with one broken bar, and motor with two broken bars. (a) MCSA and (b) proposed methodology.

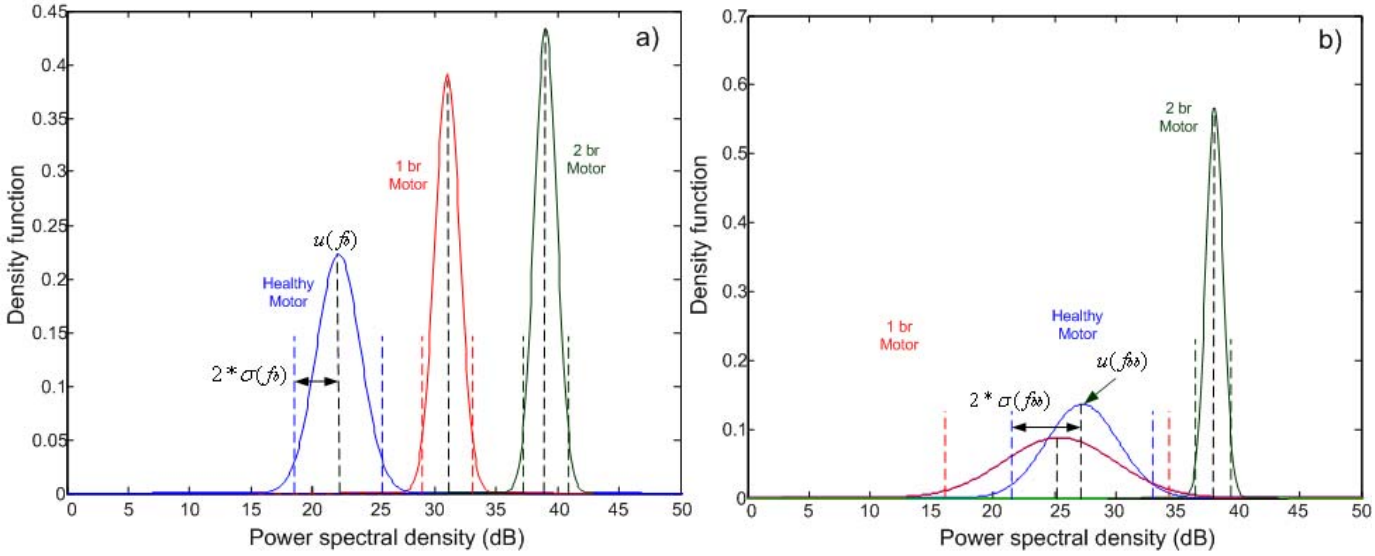

Fig. 7. Statistical analysis for a mechanical load of 100%. (a) Proposed methodology, f_b and (b) analysis in f_{bb}.

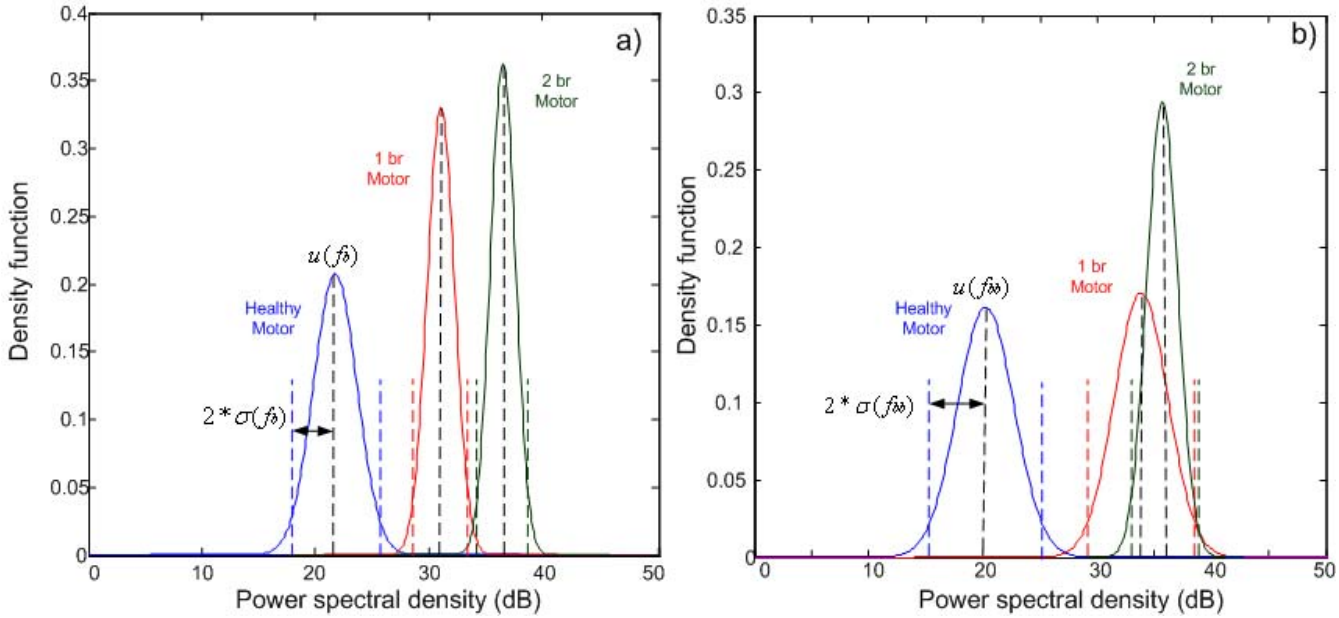

Fig. 8. Statistical analysis for a mechanical load of 75%. (a) Proposed methodology, f_b and (b) analysis in f_{bb}.

This process is taken into consideration the slip of the motor. The selection is done as follows: if region A_4 has the biggest amplitude then motor has full load, ifA_3 has the biggest amplitude then the motor has 75% and so on. This process is carried out in the load condition unit.

8) Once the load condition is determined, the resultant amplitude of the corresponding area is sent to the decision-making unit for threshold comparison as proposed in [21]. The decision-making unit is composed of a decision tree in which the thresholds obtained for each condition motor are compared with the resultant amplitude A_{s} to determine the motor condition. Fig. 5 shows the implementation of the decision-making unit, the threshold blocks contains the lower and upper limits for each condition, these limits are: *hL* is a lower limit and *hH* is an upper limit for healthy motor, *1bL* and *2bH* are the lower and upper limits for one broken bar, respectively, and *2bL* and *2bH* are the lower and upper limits for two broken bars, respectively.

The decision-making unit states the motor condition by indicating whether the motor is in good condition or in a broken bars condition.

IV. Testing Results and Analysis

To assess the detection improvement of the proposed methodology a statistical analysis was performed. Two sets of three 1-HP induction motors at different load condition were used for the tests. Each motor was tested under four different load conditions: 25%, 50%, 75%, and 100%. 50 runs

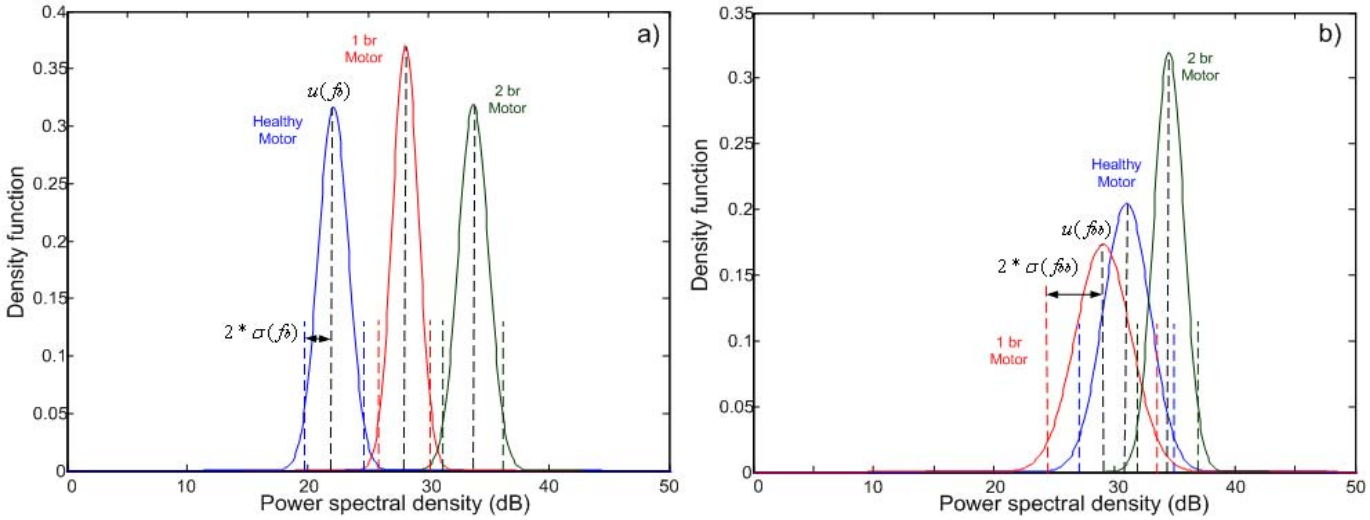

Fig. 9. Statistical analysis for a mechanical load of 50%. (a) Proposed methodology, f_b and (b) analysis in f_{bb}.

in each load condition were analyzed. The bar breakage was done by externally drilling the rotor. The motors are classified into healthy, one broken bar, and two broken bars, respectively. In each case, several tests using different structural element sizes were carried out; the best result was obtained using a structural element size equal to five points. Fig. 4 shows an example of the spectra of dilation signals for a healthy motor (a), a motor with one broken bar (b), and a motor with two broken bars (b). A comparison among Fig. 4(a), (b), and (c) shows that different spectral components may be used for fault condition monitoring. It is clear that frequency f_{b} presents greater frequency amplitude than frequency f_{bb}, improving detectability.

Fig. 6 shows the representation of the area value for each condition using two different signal-processing methodologies. Fig. 6(a) shows power spectral densities of a healthy motor, a motor with one broken bar, and a motor with two broken bars, obtained using MCSA and the proposed methodology. The amplitude for frequency f_b, frequency f_{bb} and supply frequency f_s are presented. Although two broken bar failure is scarce detectable, one broken bar failure is difficult to detect. The spurious frequency increases its value in both frequencies f_b and f_{bb}. Fig. 5(b) shows the spectra of a healthy motor, a motor with one broken bar, and a motor with two broken bars using the proposed methodology. Faulty condition can be detected in both frequencies f_b and f_{bb}; however, frequency f_b shows greater amplitude improving the detectability. A comparison between Fig. 6(a) and (b) shows how the proposed methodology improves the detectability of a broken bar.

The results of the statistical analysis for a mechanical load of 100%, 75%, 50%, and 25%, are shown in Figs. 7–10 respectively, where $\mu(f_b)$ is the mean of f_b, $\sigma(f_b)$ the standard deviation, $\mu(f_{\mathrm{bb}})$ is then mean of the f_{bb} and $\sigma(f_{\mathrm{bb}})$ the standard deviation. Fig. 7(a) shows a plot of the Gaussian distribution of the 50 runs for each motor condition: healthy motor (blue), one broken bar (red), and two broken bars (green), considering the area A_4. The three Gaussian distributions are separated by almost three standard deviations allowing detectability of 98%. Fig. 7(b) shows the Gaussian distributions for the same conditions, but using MCSA and f_{bb}. In this case, healthy motor, and one broken bar condition are overlapped impeding the detection. It means that for full load, the application of dilation transform increases the detectability in 95% between healthy motor and one broken bar.

Fig. 8(a) shows the statistical analysis for data with 75% mechanical load. 50 runs for each motor condition were made, area A_3 was used. The figure shows a good detectability, with at least two standard deviations separation among each Gaussian distribution. One broken bar and two broken bar conditions show statistical distributions close to each other; however, the separation is enough to provide a 95% of detectability. Fig. 8(b) shows the results using f_{bb} as a detection frequency; notice that one broken bar and two broken bars condition are overlapped. For this load condition, the proposed methodology increases the detectability between one broken bar and two broken bar from 50% to 95%.

The statistical analysis for data with 50% mechanical load is shown in Fig. 9. The results of the proposed methodology for this condition are similar to the case previously described. Gaussian distributions are separated by more of two standard deviations with an accuracy of 95%. For this condition area A_2 was used. Fig. 9(b) shows an overlapping on each condition inhibiting the detection.

The last analyzed condition corresponds to the case of 25% mechanical load. The statistical analysis for this condition is shown in Fig. 10. In this case, there is an overlap between one broken bar and two broken bars distributions. In consequence, the detection between these two conditions is 60%; yet, in the case of healthy motor the detection is more than 95% due to the separation of two standard deviations. Fig. 10(b) shows an overlap among each condition inhibiting the detectability. The proposed methodology allows a detectability of 95% between healthy motor and motor with one broken bar.

Tables I and II present the broken bar criteria in decibels for the first and second set of motors, respectively. Tables I and II show the conditions described in this paper:

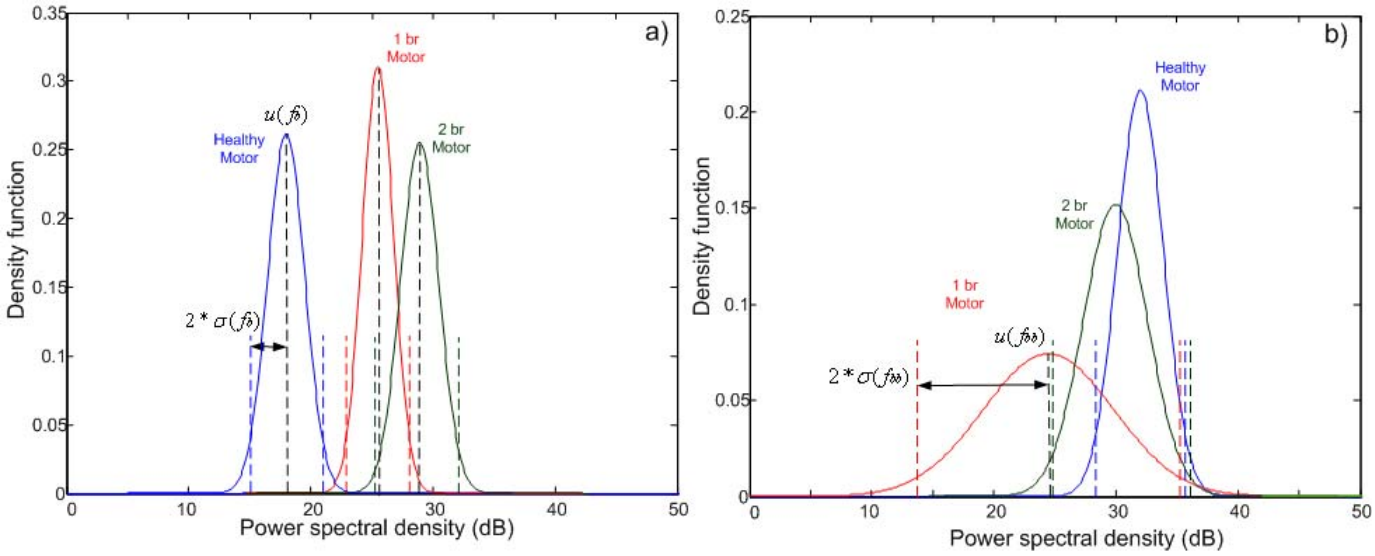

Fig. 10. Statistical analysis for a mechanical load of 25%. (a) Proposed methodology, fb and (b) analysis in fbb.

TABLE I
BROKEN BAR CRITERIA IN DECIBELS FOR THE FIRST SET OF MOTORS

Proposed Methodology f_b				MCSA f_{bb}	
Motor condition		$\mu(f_b)$	$\sigma(f_b)$	$\mu(f_{bb})$	$\sigma(f_{bb})$
Healthy	100%	22.0459	1.78815	27.1820	2.9303
One broken bar	100%	30.9130	1.0207	25.304	4.5365
Two broken bar	100%	38.9243	0.9191	37.9438	0.7025
Healthy	75%	21.6724	1.9248	20.1252	2.4695
One broken bar	75%	30.9910	1.20785	33.7266	2.3342
Two broken bar	75%	36.4689	1.1002	35.5791	1.3539
Healthy	50%	22.0241	1.259	30.9237	1.9474
One broken bar	50%	28.0159	1.0764	28.9653	2.3011
Two broken bar	50%	33.6565	1.25155	34.4312	1.2481
Healthy	25%	17.8884	1.5238	31.9096	1.8873
One broken bar	25%	25.3989	1.28275	24.3858	5.3730
Two broken bar	25%	28.8170	1.56175	29.8649	2.6238

TABLE II
BROKEN BAR CRITERIA IN DECIBELS FOR THE SECOND SET OF MOTORS

Proposed Methodology f_b				MCSA f_{bb}	
Motor condition		$\mu(f_b)$	$\sigma(f_b)$	$\mu(f_{bb})$	$\sigma(f_{bb})$
Healthy	100%	22.0459	1.78815	27.1820	2.9303
One broken bar	100%	30.9130	1.0207	25.304	4.5365
Two broken bar	100%	38.9243	0.9191	37.9438	0.7025
Healthy	75%	21.6724	1.9248	20.1252	2.4695
One broken bar	75%	30.9910	1.20785	33.7266	2.3342
Two broken bar	75%	36.4689	1.1002	35.5791	1.3539
Healthy	50%	22.0241	1.259	30.9237	1.9474
One broken bar	50%	28.0159	1.0764	28.9653	2.3011
Two broken bar	50%	33.6565	1.25155	34.4312	1.2481
Healthy	25%	17.8884	1.5238	31.9096	1.8873
One broken bar	25%	25.3989	1.28275	24.3858	5.3730
Two broken bar	25%	28.8170	1.56175	29.8649	2.6238

healthy motor, one broken bar motor, and two broken bars motor under different mechanical load, showing the statistical values mean $\mu(f_b)$ and standard deviation $\sigma(f_b)$ for each case. The corresponding values of $\mu(f_{\text{bb}})$ and $\sigma(f_{\text{bb}})$ are also presented in Tables I and II. The median and standard deviation values show the detection condition of the proposed methodology for several mechanical load and motor conditions, where MCSA has low detection accuracy and, therefore, it is not possible to detect the motor condition.

V. CONCLUSION

Mathematical morphology was used to improved MCSA analysis to detect broken rotor bars in early stages. Spurious frequencies associated with broken bar conditions are emphasized through a morphologic dilation transform, which improves the detection with an automatic system. Figs. 7–10 show comparative statistics obtained with typical MCSA analysis and the proposed method. Gaussian distribution corresponding to both cases shows how the conditions separability is increased when the proposed method is applied. The statistical analysis summarized in Tables I and II demonstrated the detection accuracy of the proposed methodology.

An FPGA-based methodology to enhance detectability for broken bar detection under different load condition using MCSA and MM was presented. The current signal was obtained from a single phase by a standard clamp. The implementation was made into an FPGA from Altera to achieve online operation. Selected frequency f_b for analysis shows better detection than frequency f_{bb} when the signal is preprocessed by dilation transformation. In addition with the preprocessing stage, the load detection can be made. Load detection consist of a comparison among four analysis areas; these areas increase their amplitude when the failure is presented, if no failure is presented the healthy area has the biggest amplitude. Efficiency of the proposed methodology was verified through extensive experimentation with 400 runs for each motor condition: healthy, one broken bar, and two broken bar. These 400 runs were divided in eight sets of 100 runs for 25%, 50%, 75%, and 100% mechanical load.

Tables I and II show similar values demonstrating the detection accuracy of the proposed methodology. The proposed methodology has an accuracy of 95% for all conditions, remarking that in the case of 25% load the methodology was able to separate two conditions: healthy motor and failure motor. Different motor faults will be considered in a future work.

REFERENCES

[1] S. Toscani, M. Faifer, M. Rossi, L. Cristaldi, and M. Lazzaroni, "Effects of the speed loop on the diagnosis of rotor faults in induction machines," *IEEE Trans. Instrum. Meas.*, vol. 61, no. 10, pp. 2713–2722, Oct. 2012.

[2] R. Puche-Panadero, M. Pineda-Sanchez, M. Riera-Guasp, J. Roger-Folch, E. Hurtado-Perez, and J. Perez-Cruz, "Improved resolution of the MCSA method via hilbert transform, enabling the diagnosis of rotor asymmetries at very low slip," *IEEE Trans. Energy Convers.*, vol. 24, no. 1, pp. 52–59, Mar. 2009.

[3] J. Cusido, L. Romeral, A. Garcia, J. Ortega, and J. Riba, "On-line fault detection method for induction machines based on signal convolution," *Eur. Trans. Electr. Power*, vol. 21, no. 1, pp. 475–488, 2011.

[4] A. Jawadekar, M. Dhole, and S. Paraskar, "Signal processing based wavelet approach for fault detection of induction motor," *Int. J. Sci. Spirituality Bus. Technol.*, vol. 1, no. 1, pp. 70–75, Mar. 2012.

[5] M. Pineda-Sanchez, M. Riera-Guasp, J. A. Antonino-Daviu, J. Roger-Folch, J. Perez-Cruz, and R. Puche-Panadero, "Diagnosis of induction motor faults in the fractional fourier domain," *IEEE Trans. Instrum. Meas.*, vol. 59, no. 8, pp. 2065–2075, Aug. 2010.

[6] A. Garcia-Perez, R. Romero-Troncoso, E. Cabal-Yepez, R. Osornio-Rios, J. Rangel-Magdaleno, and H. Miranda, "Startup current analysis of incipient broken rotor bar in induction motors using high-resolution spectral analysis," in *Proc. IEEE Int. Symp. Diag. Electr. Mach. Power Electron. Drives*, Sep. 2011, pp. 657–663.

[7] A. Ordaz-Moreno, R. J. Romero-Troncoso, J. Vite-Frias, J. R. Rivera-Guillen, and A. Garcia-Perez, "Automatic online diagnosis algorithm for broken-bar detection on induction motors based on discrete wavelet transform for FPGA implementation," *IEEE Trans. Ind. Electron.*, vol. 55, no. 5, pp. 2193–2202, May 2008.

[8] J. Rangel-Magdaleno, H. Peregrina-Barreto, and J. Ramirez-Cortes, "Broken bars detection on induction motor using MCSA and mathematical morphology: An experimental study," in *Proc. IEEE Int. Conf. Instrumt. Meas.*, May 2013, pp. 825–829.

[9] H. Keskes, A. Braham, and Z. Lachiri, "Broken rotor bar diagnosis in induction machines through stationary wavelet packet transform and multiclass wavelet SVM," *Electr. Power Syst. Res.*, vol. 97, pp. 151–157, Apr. 2013.

[10] L. Eren and M. J. Devaney, "Effect of current resampling in motor current signature analysis," in *Proc. IEEE Int. Conf. Instrum. Meas.*, May 2013, pp. 345–348.

[11] L. Cristaldi, M. Faifer, M. Lazzaroni, and S. Toscani, "An inverter-fed induction motor diagnostic tool based on time-domain current analysis," *IEEE Trans. Instrum. Meas.*, vol. 58, no. 5, pp. 1454–1461, May 2009.

[12] M. Riera-Guasp, M. Pineda-Sanchez, J. Perez-Cruz, R. Puche-Panadero, J. Roger-Folch, and J. A. Antonino-Daviu, "Diagnosis of induction motor faults via gabor analysis of the current in transient regime," *IEEE Trans. Instrum. Meas.*, vol. 61, no. 6, pp. 1583–1596, Jun. 2012.

[13] B. M. Ebrahimi, A. M. Takbash, and J. Faiz, "Losses calculation in line-start and inverter-fed induction motors under broken bar fault," *IEEE Trans. Instrum. Meas.*, vol. 62, no. 1, pp. 140–152, Jan. 2013.

[14] A. Sadeghian, Z. Ye, and B. Wu, "Online detection of broken rotor bars in induction motors by wavelet packet decomposition and artificial neural networks," *IEEE Trans. Instrum. Meas.*, vol. 58, no. 7, pp. 2253–2263, Jul. 2009.

[15] N. Q. Hu, L. R. Xia, F. S. Gu, and G. J. Qin, "A novel transform demodulation algorithm for motor incipient fault detection," *IEEE Trans. Instrum. Meas.*, vol. 60, no. 2, pp. 480–487, Feb. 2011.

[16] G. Betta, C. Liguori, A. Paolillo, and A. Pietrosanto, "A DSP-based FFT-analyzer for the fault diagnosis of rotating machine based on vibration analysis," *IEEE Trans. Instrum. Meas.*, vol. 51, no. 6, pp. 1316–1322, Dec. 2002.

[17] J. J. Rangel-Magdaleno, R. J. Romero-Troncoso, R. Osornio-Rios, E. Cabal-Yepez, and A. Dominguez-Gonzalez, "FPGA-based vibration analyzer for continuous CNC machinery monitoring with fused FFT-DWT signal processing," *IEEE Trans. Instrum. Meas.*, vol. 59, no. 12, pp. 3184–3194, Dec. 2012.

[18] D. Bayram and S. Seker, "Wavelet based neuro-detector for low frequencies of vibration signals in electric motors," *Appl. Soft Comput.*, vol. 13, no. 5, pp. 2683–2691, 2013.

[19] C. da Costa, M. Mathias, P. Ramos, and P. Silva, "A new approach for real time fault diagnosis in induction motors based on vibration measurement," in *Proc. IEEE Instrum. Meas. Technol. Conf.*, May 2012, pp. 1164–1168.

[20] L. Contreras-Medina, R. J. Romero-Troncoso, J. R. Millan-Almaraz, and C. Rodriguez-Donate, "FPGA based multiple-channel vibration analyzer embedded system for industrial applications in automatic failure detection," in *Proc. Symp. Ind. Embedded Syst.*, Jun. 2008, pp. 229–232.

[21] J. Rangel-Magdaleno, R. Romero-Troncoso, R. Osornio-Rios, E. Cabal-Yepez, and L. Contreas-Medina, "Novel methodology for online half-broken-bar detection on induction motors," *IEEE Trans Instrum. Meas.*, vol. 58, no. 5, pp. 1690–1698, May 2009.

[22] Y. Gritli, A. Di Tommaso, F. Filippetti, R. Miceli, C. Rossi, and A. Chatti, "Investigation of motor current signature and vibration analysis for diagnosing rotor broken bars in double cage induction motors," in *Proc. Int. Symp. Power Electron. Electr. Drives, Autom. Motion*, Jun. 2012, pp. 1360–1365.

[23] B. M. Ebrahimi, J. Faiz, and B. Akin, "Pattern recognition for broken bars fault diagnosis in induction motors under various supply conditions," *Eur. Trans. Electr. Power*, vol. 22, no. 8, pp. 1176–1190, 2011.

[24] M. R. Mehrjou, N. Mariun, M. H. Marhaban, and N. Misron, "Rotor fault condition monitoring techniques for squirrel-cage induction machine—A review," *Mech. Syst. Signal Process.*, vol. 25, no. 8, pp. 2827–2848, Nov. 2011.

[25] M. Cabanas, F. Pedrayes, M. Melero, C. Rojas-Garcia, J. Cano, G. Orcajo, *et al.*, "Unambiguous detection of broken bars in asynchronous motors by means of a flux measurement-based procedure," *IEEE Trans. Instrum. Meas.*, vol. 60, no. 3, pp. 891–899, Mar. 2011.

[26] J. Serra, *Image Analysis and Mathematical Morphology*. New York, NY, USA: Academic, 1982.

[27] P. Soille, *Morphological Image Analysis: Principles and Applications*. New York, NY, USA: Springer-Verlag, 2003.

[28] T. Radil, P. M. Ramos, F. M. Janeiro, and A. Cruz-Serra, "PQ monitoring system for real-time detection and classification of disturbances in a single-phase power system," *IEEE Trans. Instrum. Meas.*, vol. 57, no. 8, pp. 1725–1733, Aug. 2008.

[29] M. Jing, X. Yan, W. Zengping, and L. Haofang, "A novel adaptive scheme of discrimination between internal faults and inrush currents of transformer using mathematical morphology," in *Proc. IEEE Power Eng. Soc. General Meeting*, Jun. 2006, pp. 1–7.

Jose de Jesus Rangel-Magdaleno (S'08–M'12) received the B.E. degree in electronics engineering and the M.E. degree in electrical engineering from Universidad de Guanajuato, Guanajuato, Mexico, in 2006 and 2008, respectively, and the Ph.D. degree in mechatronics from Universidad Autonoma de Queretaro, Queretaro, Mexico, in 2011.

He is currently an Associate Researcher with the Electronics Department, National Institute of Astrophysics, Optics, and Electronics, Puebla, Mexico. He is a member of the Mexican National Research System (SNI), level 1. His current research interests include signal and image processing, instrumentation and mechatronics.

Hayde Peregrina-Barreto (S'09–M'12) received the B.Sc. degree from the Technological Institute of Cuautla, Cuautla, Mexico, the M.Sc. degree in engineering from the University of Guanajuato, Guanajuato, Mexico, and the Ph.D. degree in engineering from the Autonomous University of Queretaro, Queretaro, Mexico.

She is currently a Titular Researcher of Computer Science with LiCore, Queretaro, and a member of the Mexican National Research System (SNI), level C. Her current research interests include image processing include mathematical morphology, color appearance models, segmentation, and human visual perception.

Juan Manuel Ramirez-Cortes (SM'04) was born in Puebla, Mexico. He received the B.Sc. degree from the National Polytechnic Institute, Mexico City, Mexico, the M.Sc. degree from the National Institute of Astrophysics, Optics, and Electronics (INAOE), Puebla, and the Ph.D. degree from Texas Tech University, Lubbock, TX, USA, all in electrical engineering.

He is currently a Titular Researcher with the Electronics Department, INAOE. He is the President of the IEEE Puebla Section, and a member of the Mexican National Research System (SNI), level 1. His current research interests include signal and image processing, neural networks, pattern recognition, and instrumentation and sensors.

Pilar Gomez-Gil (SM'04) was born in Puebla, Mexico. She received the B.Sc. degree from the University of the Americas, Puebla, and the M.Sc. and Ph.D. degrees from Texas Tech University, Lubbock, TX, USA, all in computer science.

She is currently a Titular Researcher of Computer Science with the National Institute of Astrophysics, Optics, and Electronics, Puebla, and a member of the Mexican National Research System (SNI), level 1. Her current research interests include neural networks, signal processing, pattern recognition, and other computational intelligence techniques.

Roberto Morales-Caporal (S'05–M'08) received the B.Sc. degree in electromechanical engineering from the Technological Institute of Apizaco, Apizaco, Mexico, in 1999, the M.Sc. degree in electrical engineering from the Graduate and Research Department, Superior School of Mechanical and Electrical Engineering, National Polytechnic Institute, Mexico, in 2001, and the Dr.-Ing. degree in electrical engineering from the University of Siegen, Siegen, Germany, in 2007, with a scholarship awarded by the German Academic Exchange Service for doctoral studies in 2003.

He has been with the Postgraduate Studies and Research Division, Technological Institute of Apizaco, Apizaco, since 2008. His current research interests include motor control, sensorless control, control of power converters for renewable energy, and DSP-based digital control.

Dr. Morales-Caporal was a recipient of the IEEE Industrial Electronics Society Student Scholarship to attend the 2005 Annual Conference of the IEEE Industrial Electronics Society. He was also a recipient of the First Prize Paper Award from the Technical Committee on Electrical Machines of the IEEE Industrial Electronics Society in 2009.